# DESIGN AND IMPLEMENTATION OF THE SOLAR ANALYST: AN ARCVIEW EXTENSION FOR MODELING SOLAR RADIATION AT LANDSCAPE SCALES

by

**Pinde Fu**
Department of Geography
GEMLab/Kansas Applied Remote Sensing Program
The University of Kansas

**Paul Rich**
Department of Ecology & Evolutionary Biology
Kansas Biological Survey
& Environmental Studies Program
The University of Kansas

**Citation:**
Fu, P. and P.M. Rich. 1999. Design and implementation of the Solar Analyst: an ArcView extension for modeling solar radiation at landscape scales. Proceedings of the Nineteenth Annual ESRI User Conference

## ABSTRACT

Incoming solar radiation (insolation) is the primary driving force for Earth's physical, biological, and industrial systems. Knowledge of the amount of insolation at various geographic locations is desirable for application in such diverse fields as solar energy utilization, civil engineering, agriculture, forestry, meteorology, environmental assessment, and ecological research. For most geographical areas, however, insolation data are not available. Simple interpolation and extrapolation of point–specific measurements are typically not feasible, because insolation can vary significantly within short distances due to topographic heterogeneity and nearground features. While some geographical information systems (GIS) based solar radiation modeling capabilities have been developed, there is a need for expanded functionality, accuracy, and calculation speed. We developed the Solar Analyst as an ArcView GIS extension, using C++, Avenue, and the GridIO library. The Solar Analyst is a comprehensive geometric solar radiation modeling tool. It calculates insolation maps using digital elevation models (DEMs) for input. Highly optimized algorithms account for the influences of the viewshed, surface orientation, elevation, and atmospheric conditions. The Solar Analyst model was validated by comparing calculated temporal and spatial patterns of insolation in the vicinity of Rocky Mountain Biological Laboratory (RMBL) with detailed monitoring of insolation, weather, and vegetation.

The Solar Analyst provides a convenient and effective tool for understanding spatial and temporal variation of insolation at landscape and local scales.

## 1. INTRODUCTION: SPATIAL SOLAR RADIATION MODELS

### 1.1 Importance of Understanding Landscape Patterns of Solar Radiation

Incoming solar radiation (insolation), with a continual input of 170 billion megawatts to the earth, is the primary driver for our planet's physical and biological processes (Geiger 1965, Gates 1980, Dubayah and Rich 1995, 1996). Almost all human activities (agriculture, forestry, building design, and land management) ultimately depend upon insolation. At a global scale, the latitudinal gradients of insolation, caused by the geometry of Earth's rotation and revolution about the sun, are well known. At the landscape scale, topography is the major factor modifying the distribution of insolation. Variability in elevation, surface orientation (slope and aspect), and shadows cast by topographic features create strong local gradients of insolation. This leads to high spatial and temporal heterogeneity in local energy and water balance, which determines microenvironmental factors such as air and soil temperature regimes, evapotranspiration, snow melt patterns, soil moisture, and light available for photosynthesis. These factors in turn affect the spatial patterning of natural processes and human endeavor. Accurate insolation maps at landscape scales are desired for many applications. Although there are thousands of solar radiation monitoring locations throughout the world (many associated with weather stations), for most geographical areas accurate insolation data are not available. Simple interpolation and extrapolation of point–specific measurements to areas are generally not meaningful because most locations are affected by strong local variation. Accurate maps of insolation would require a dense collection station network, which is not feasible because of high cost. Spatial solar radiation models provide a cost-efficient means for understanding the spatial and temporal variation of insolation over landscape scales (Dubayah and Rich 1995, 1996). Such models are best made available within a geographic information system (GIS) platform, whereby insolation maps can be conveniently generated and related to other digital map layers.

### 1.2 Spatial Solar Radiation Models

Spatial insolation models can be categorized into two types: point specific and area based. Point-specific models compute insolation for a location based upon the geometry of surface orientation and visible sky. The local effect of topography is accounted for by empirical relations (Buffo et al. 1972, Frank and Lee 1966, Kondrtyev 1969), by visual estimation (Swift 1976, Flint and Childs 1987), or, more accurately, by the aid of upward-looking hemispherical (fisheye) photographs (Rich 1989, 1990, Rich et al. 1999). Point-specific models can be highly accurate for a given location, but it is not feasible to build a specific model for each location over a landscape. In contrast, area-based models compute insolation for a geographical area, calculating surface orientation and shadow effects from a digital elevation model (DEM) (Hetrick et al. 1993a, 1993b, Dubayah and Rich 1995, 1996, Rich et al. 1995, Kumar et al. 1997). These models provide important tools for understanding landscape processes. The SolarFlux model (Hetrick et al. 1993a, 1993b, Rich et al. 1995), developed for use within the ARC/INFO GIS platform (Environmental Systems Research Institute [ESRI], Redlands, CA), simulates the

influence of shadow patterns on direct insolation using the ARC/INFO Hillshade function at discrete intervals through time. SolarFlux was implemented in the Arc Macro Language (AML), which strongly limits its computation speed and its accessibility. Kumar et al. (1997) developed a similar model using ARC/INFO and the GENAMAP GIS software (GENASIS, Australia). Whereas point-specific models can be highly accurate for a specific location, area-based models can calculate insolation for every location over a landscape. A new generation of spatial models is needed that combines these respective advantages, providing rapid and accurate maps of insolation over landscape scales.

### 1.3 Features of the Solar Analyst

Herein we describe the design and implementation of the Solar Analyst, a spatial solar radiation model implemented as an ArcView GIS (ESRI) extension. TopoView is a counterpart of the Solar Analyst implemented to run in the Arc/Info GIS platform (ESRI) rather than in ArcView. Except for some details of the user interface, the following discussion applies to both the Solar Analyst and TopoView. First we explain the underlying theory, design considerations, and implementation of the Solar Analyst. Then, we validate the Solar Analyst by comparing simulations with temporal and spatial analyses of empirical data from the vicinity of Rocky Mountain Biological Laboratory (RMBL). Finally, we explore the application of the Solar Analyst to examine landscape patterns of insolation. The Solar Analyst draws from the strengths of both point-specific and area-based models. In particular, the Solar Analyst generates an upward-looking hemispherical viewshed, in essence producing the equivalent of a hemispherical (fisheye) photograph (Rich 1989, 1990) for every location on a DEM. The hemispherical viewsheds are used to calculate the insolation for each location and produce an accurate insolation map. The Solar Analyst can calculate insolation integrated for any time period. It accounts for site latitude and elevation, surface orientation, shadows cast by surrounding topography, daily and seasonal shifts in solar angle, and atmospheric attenuation. The Solar Analyst has the following advantages over previously developed models:

- **versatile outputs:** creates maps of direct, diffuse, global radiation, and direct radiation duration for any period (instantaneous, daily, monthly, biweekly …); also calculates skyview factors, sunmaps and skymaps, viewsheds, and horizon angles; analyses can be performed for whole DEMs, restricted areas, or specific cells;
- **simple input:** uses digital elevation models (DEMs) and a few readily available parameters;
- **fast and accurate:** uses an advanced viewshed algorithm for calculations;
- **easy to use & broad accessibility:** based in ArcView, which supplies the Solar Analyst with mapping, query, graphing, and statistical analysis functions in a powerful desktop GIS platform.

## 2. THEORY, DESIGN, AND IMPLEMENTATION OF THE SOLAR ANALYST

### 2.1 Theory: Use of Hemispherical Viewsheds in Solar Radiation Models

**Hemispherical Viewshed Algorithm:** Solar Radiation originating from the sun travels through the atmosphere, is modified by topography and other surface features, and then is intercepted as direct, diffuse, and reflected insolation components. Generally, direct radiation is the largest component of total radiation, and diffuse radiation is the second largest component. Radiation reflected to a location from surrounding topographic features generally accounts for a small proportion of total incident radiation and for many purposes can be neglected (Gates 1980, Rich 1989, 1990, Hetrick et al. 1993a, 1993b, Kumar 1997). Rich (1994) developed an algorithm for rapid insolation calculation which, until now, has only been partially implemented in point-specific models including Canopy (Rich 1989, 1990) and Hemiview software (Rich et al. 1999) used for analysis of hemispherical photography. This hemispherical viewshed algorithm serves as the core of the Solar Analyst.

**Viewshed Calculation:** Viewsheds are calculated for each cell of the input DEM. A viewshed is the angular distribution of sky obstruction. This is similar to the view provided by upward-looking hemispherical (fisheye) photographs. A viewshed is calculated by searching in a specified set of directions around a location of interest (Fig. 1A), determining the maximum angle of sky obstruction, also referred to as horizon angle, in each direction (Fig. 1B)(Dozier and Frew 1990). For other unsearched directions, horizon angles are calculated using interpolation (Fig. 1C). Then the horizon angles are converted into a hemispherical coordinate system, in particular utilizing an equiangular hemispherical projection, which represents a three-dimensional hemisphere of directions as a two-dimensional grid (Fig. 1D). The resolution of the viewshed grid must be sufficient to adeduately represent all sky directions, but small enough to enable rapid calculations, e.g., 200 x 200 cells, 512 x 512 cells. Each grid cell is assigned a value that corresponds with visible versus obstructed sky directions. The grid cell location, row and column, corresponds to a zenith angle q (angle relative to the zenith) and an azimuth angle a (angle relative to north) on the hemisphere of directions.

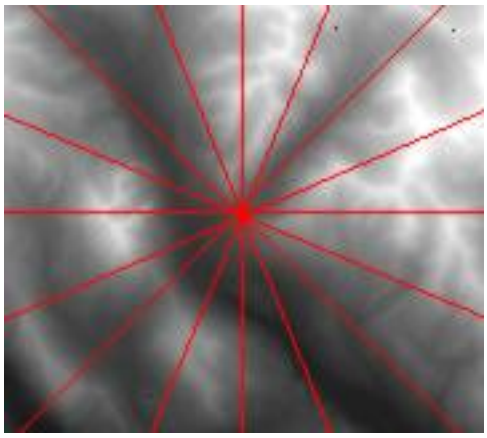

1A) Horizon angles are traced along a specified set of directions.

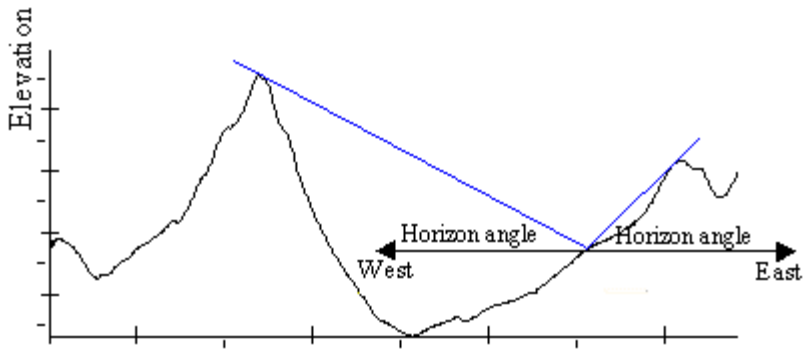


1B) Horizon angles are calculated for each direction.

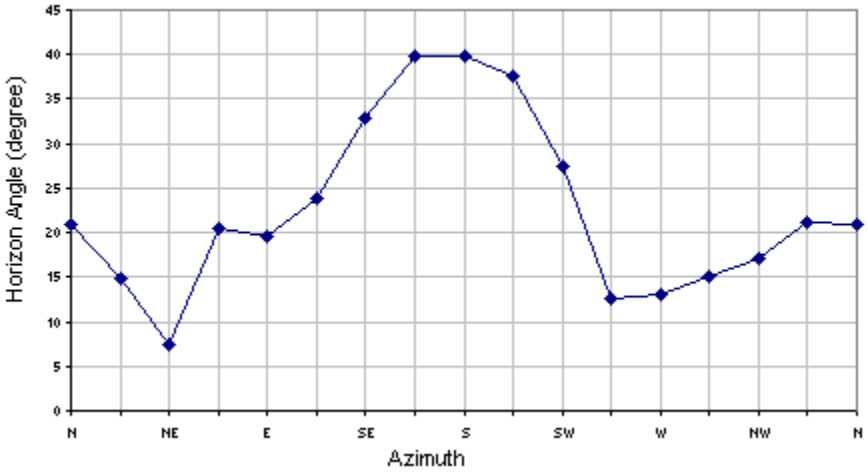


1C) Horizon angles are interpolated for all directions.

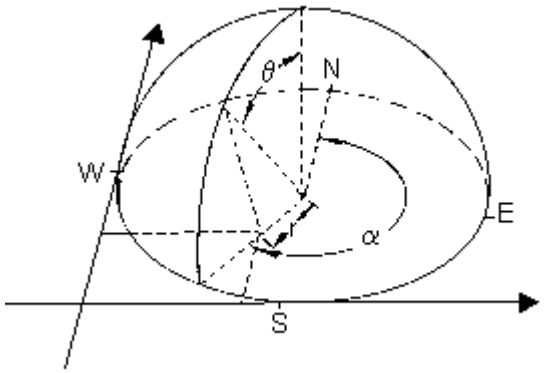


1D) Horizon angles are converted to a hemispherical coordinate system.

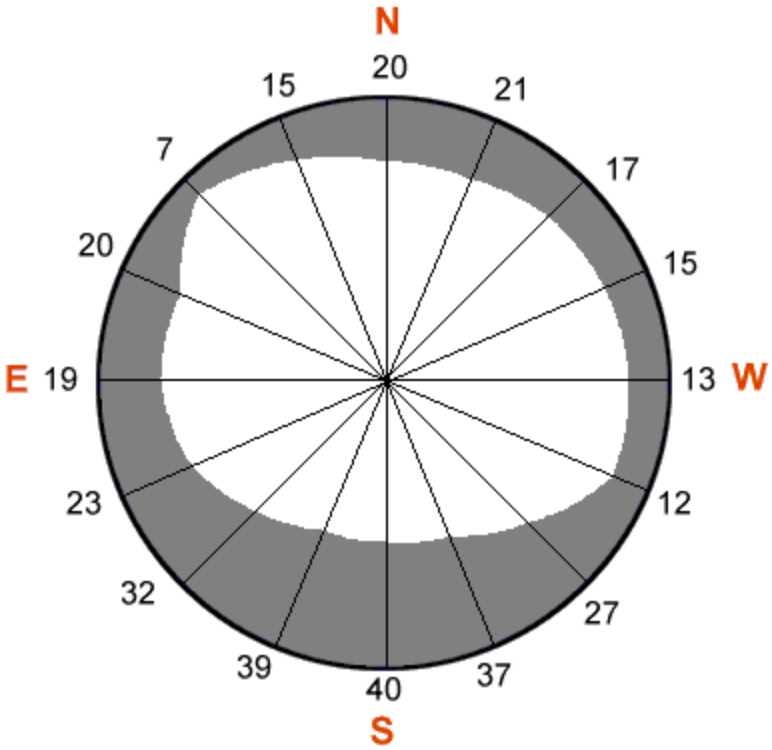


1E) The resulting viewshed for a location represents which sky directions are visible and which are obscured. Numbers represent the calculated horizon angles.

Fig 1. Calculation of the viewshed for one cell of a DEM.

**Sunmap Calculation:** The amount of direct solar radiation originating from each sky direction is represented by creating a sunmap in the same hemispherical projection as for the viewshed (Fig. 2). The skymap specifies suntracks, the apparent position of the sun as it varies through time. In particular, suntracks are represented by discrete sky sectors, defined by sun position at intervals through the day and season (e.g., half-hour intervals through the day and month intervals through the season). The position of the sun (zenith and azimuth angles) is calculated based on latitude, day of year, and time of day using standard astronomical formulae (modified version of Gates 1980). Zenith and azimuth angles are projected into two-dimensional grids with the same resolution used for viewsheds. Two sunmaps are created, one to represent periods between the winter solstice and the summer solstice (December 22 to June 22) and the other to represent periods between the summer solstice and the winter solstice (June 22 to December 22). Each sky sector of the sunmap is flood-filled with a unique identification number. For each sector, the time duration, the azimuth and zenith at its centroid are calculated. This calculation also accounts for partial sectors near the horizon.

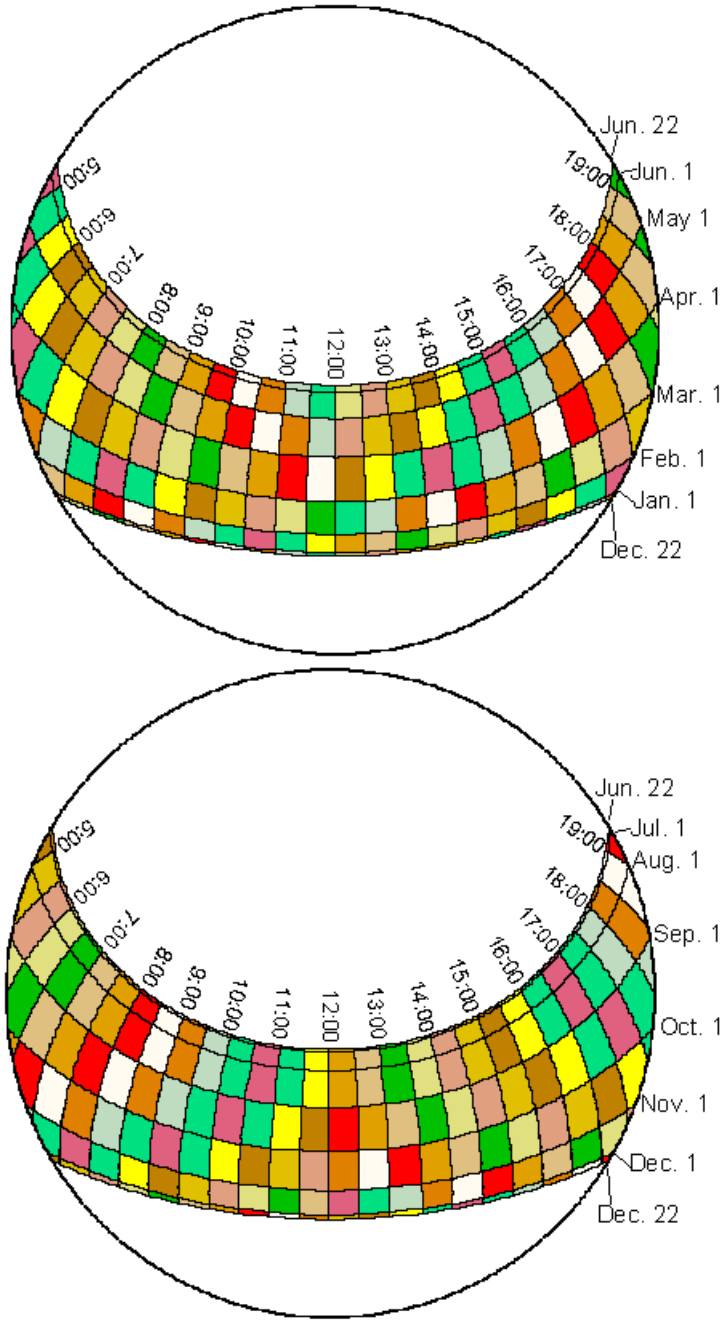


Fig. 2. Annual sunmaps for 39$^{o}$ N latitude using 0.5 hour intervals through the day and month intervals through the year.

**Penumbral Effects:** For sunmaps that represent one day or less, penumbral effects must be taken into account. The Solar Analyst uses a solar disc semidiameter of 0.00466 radians near the zenith (0.2668o) and larger values near the horizon (up to 1.6o) (U.S. Department of Energy 1978) (Fig. 3). The solar disc appears larger near the horizon due to refraction but it does not differ significantly from 0.5o after the sun has risen above an elevation angle of approximately 10o.

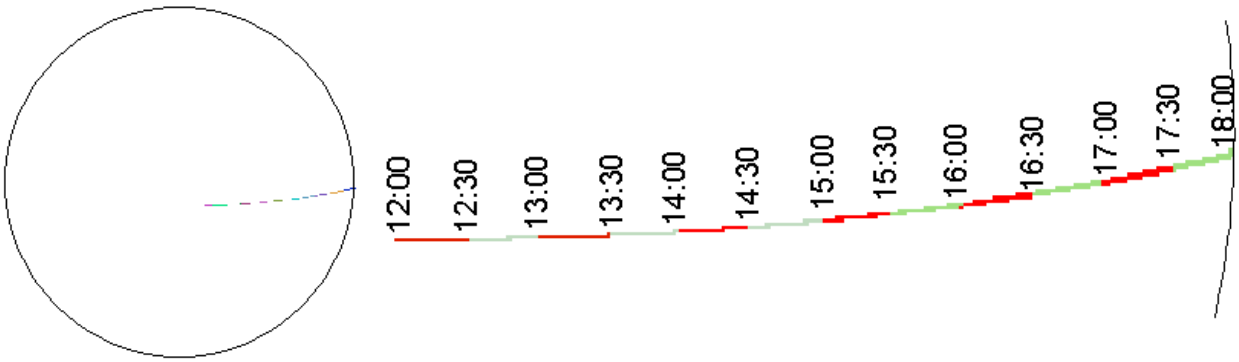


Fig. 3. Penumbral effects are accounted for by constructing sunmaps with consideration of the solar disc size. Note that the sun track becomes wider near the horizon due to refraction.

**Skymap Calculation:** Unlike direct insolation, which only originates from directions along the suntrack, diffuse solar radiation can originate from any sky direction. Skymaps are constructed by dividing the whole sky into a series of sky sectors defined by zenith and azimuth divisions. Each sector is flood-filled with a unique identification number (Fig. 4). The zenith and azimuth angles of the centroid of each sector are calculated. Sky sectors must be small enough that the centroid zenith and azimuth angles reasonably represent the direction of the sky sector in subsequent calculations (e.g., sky sectors representing $5.625^{o}$ zenith intervals [16 zenith divisions] and $22.5^{o}$ azimuth intervals [16 azimuth divisions]).

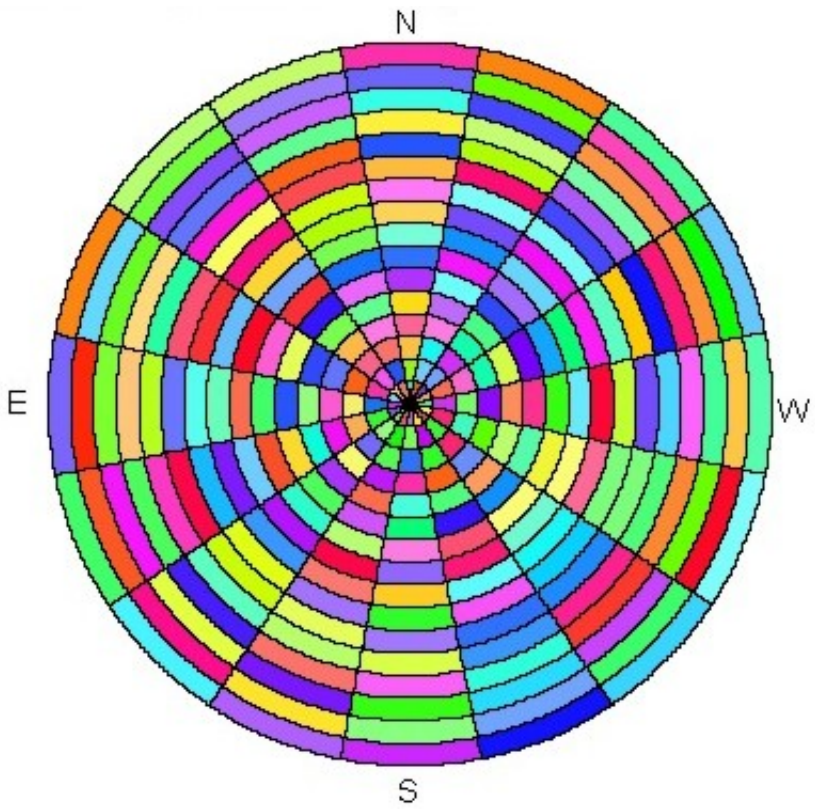


Fig. 4. A skymap with sky sectors defined by 16 zenith divisions and 16 azimuth divisions.

**Overlay of Viewsheds with Sunmaps and Skymaps:** The skymap and sunmaps are overlaid on the viewshed (Figure 5). Gap fraction, the proportion of unobstructed sky area in each skymap or sunmap sector, is calculated by dividing the number of unobstructed cells by the total number of cells in that sector.

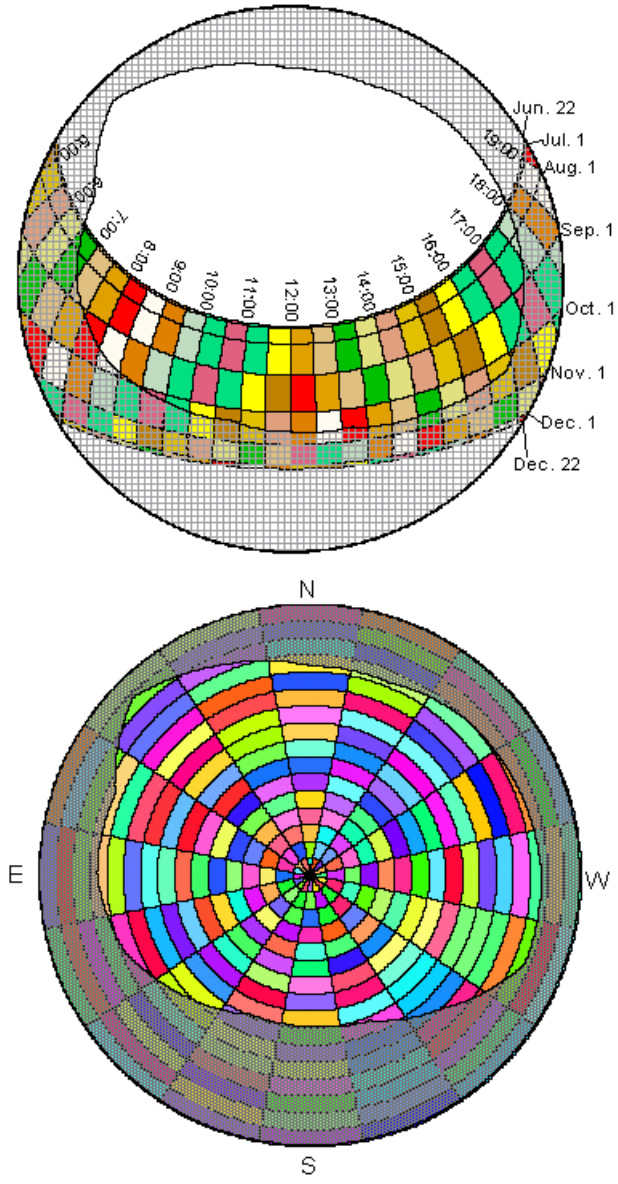


Fig 5. Overlay of a viewshed on a sunmap (upper) and a skymap (lower).
Shaded areas are obstructed sky directions.

**Direct Solar Radiation Calculation:** For each sunmap sector that is not completely obstructed, solar radiation is calculated based on gap fraction, sun position, atmospheric attenuation and ground receiving surface orientation. A simple transmission model (Rich 1989, 1990, Pearcy 1989, Monteith and Unsworth 1990, Gates 1980, List 1971), which starts with the solar constant and accounts for atmospheric effects based on transmittivity and air mass depth, is implemented using the following equations.

$$\mathbf{Dir_{tot} = \Sigma Dir_{\theta,\alpha}} \qquad \mathbf{(1)}$$

Total direct insolation ($\mathbf{Dir_{tot}}$) for a ground location is the sum of the direct insolation ($\mathbf{Dir_{\theta,\alpha}}$) from all sunmap sectors. The direct insolation from the sunmap sector with a centroid at zenith angle $\theta$ and azimuth angle $\alpha$ is calculated using equation 2.

$$\mathbf{Dir_{\theta,\alpha} = S_{Const} * \tau^{m(\theta)} * SunDur_{\theta,\alpha} * SunGap_{\theta,\alpha} * \cos(AngIn_{\theta,\alpha})} \qquad \mathbf{(2)}$$

where:

$\mathbf{S_{Const}}$ is the solar flux outside the atmosphere at the mean earth-sun distance, know as solar constant. Estimates of the solar constant range from 1338 to 1368 $WM^{-2}$. As a result of more precise measurements, the Commission for Instruments and Methods of Observation in 1981 agreed to adopt the World Radiation Center (WRC) solar constant (1367 $WM^{-2}$), as is used in the Solar Analyst. Solar constant fluctuates slightly, a few tenths of a percentage over periods of years (Iqbal 1983), and this can be accounted for by differences in the distance between the earth and sun from the mean earth-sun distance;

$\tau$ is transmittivity of the atmosphere (averaged over all wavelengths) for the shortest path (in the direction of the zenith);

**m($\theta$)** is the relative optical path length (measured relative to the zenith path length). It is determined by the solar zenith angle and elevation above sea level. For zenith angles less than $80^o$, it can be calculated using equation 3, below. For zenith angles greater than $80^o$ refraction is important. Various astronomical tables provide corrections for refraction at zenith angles greater than $80^o$ (e.g., List 1971, Table 137; Monteith and Unsworth 1990, p. 40).

$\mathbf{SunDur_{\theta,\alpha}}$ is the time duration represented by the sky sector. For most sectors, it is equal to the day interval multiplied by the hour interval. For partial sectors (near the horizon), the duration is calculated using spherical geometry;

$\mathbf{SunGap_{\theta,\alpha}}$ is the gap fraction for the sunmap sector;

$\mathbf{AngIn_{\theta,\alpha}}$ is the angle of incidence between the centroid of the sky sector and the axis normal to the surface. It can be calculated using equation 4, below. The effect of surface orientation is accounted for by multiplying by the cosine of the angle of incidence.

$$\mathbf{m = EXP(-0.000118 * Elev - 1.638 * 10^{-9} * Elev^2) / \cos(\theta)} \qquad \mathbf{(3)}$$

where:

**m** is relative optical path length;

$\theta$ is the solar zenith angle;

**Elev** is elevation above sea level in meters.

$$\mathbf{AngIn}_{\theta,\alpha} = \mathbf{acos}[\mathbf{Cos}(\theta)*\mathbf{Cos}(G_z)+\mathbf{Sin}(\theta)*\mathbf{Sin}(G_z)*\mathbf{Cos}(\alpha-G_a)] \quad (4)$$

where:

$\mathbf{AngInSky}_{\theta,\alpha}$ is the angle of incidence between the intercepting surface and a given sky sector with a centroid at zenith angle $\theta$ and azimuth angle $\alpha$;

$G_z$ is the surface zenith angle;

$G_a$ is the surface azimuth angle.

**Diffuse Solar Radiation Calculation:** For diffuse radiation the uniform diffuse model and the standard overcast diffuse model are typically implemented (Rich 1989, 1990, Pearcy 1989) with satisfactory results. In a uniform diffuse model, sometimes referred to as a "uniform overcast sky (UOC)", incoming diffuse radiation is the same from all sky directions. In a standard overcast (SOC) diffuse model, diffuse radiation flux varies with zenith angle. Both these models are implemented in the Solar Analyst. Other models can readily be implemented in the future, including anisotropic models. For each sky sector the diffuse radiation at its centroid is calculated, integrated over the time interval, and corrected by the gap fraction and angle of incidence using equation 5.

$$\mathbf{Dif}_{\theta,\alpha} = \mathbf{R}_{glb} * \mathbf{P}_{dif} * \mathbf{Dur} * \mathbf{SkyGap}_{\theta,\alpha} * \mathbf{Weight}_{\theta,\alpha} * \mathbf{cos}(\mathbf{AngIn}_{\theta,\alpha}) \quad (5)$$

where:

$\mathbf{R}_{glb}$ is the global normal radiation (see equation 6 below);

$\mathbf{P}_{dif}$ is the proportion of global normal radiation flux that is diffuse. Typically it is approximately 0.2 for clear sky conditions and ranges from 0.6 to 0.7 for very cloudy sky conditions;

**Dur** is the time interval for analysis;

$\mathbf{SkyGap}_{\theta,\alpha}$ is the gap fraction (proportion of visible sky) for the sky sector;

$\mathbf{Weight}_{\theta,\alpha}$ is proportion of diffuse radiation originating in a given sky sector relative to all sectors (see equation 7, below);

$\mathbf{AngIn}_{\theta,\alpha}$ is the angle of incidence between the centroid of the sky sector and the intercepting surface.

$\mathbf{R_{glb}}$ can be calculated by summing the direct radiation from every sector (including obstructed sector) without correction for angle of incidence, and then correcting for proportion of direct radiation, which equals to $\mathbf{1- P_{dif}}$.

$$\mathbf{R_{glb} = (S_{Const} \Sigma (\tau^{m(\theta)}) )/ (1 - P_{dif})} \qquad \mathbf{(6)}$$

For the uniform sky diffuse model, $\mathbf{Weight_{\theta,\alpha}}$ is calculated as follows:

$$\mathbf{Weight_{\theta,\alpha} = (\cos\theta_2 - \cos\theta_1) / Div_{azi}} \qquad \mathbf{(7)}$$

where:

$\theta_1$and $\theta_2$ are the bounding zenith angles of the sky sector;

$\mathbf{Div_{azi}}$ is the number of azimuthal divisions in the skymap.

For the standard overcast sky model, $\mathbf{Weight_{\theta,\alpha}}$ is calculated as follows:

$$\mathbf{Weight_{\theta,\alpha} = (2\cos\theta_2 + \cos2\theta_2 - 2\cos\theta_1 - \cos2\theta_1) / 4 * Div_{azi}} \qquad \mathbf{(8)}$$

Total diffuse solar radiation for the location ($\mathbf{Dif_{tot}}$) is calculated as the sum of the diffuse solar radiation ($\mathbf{Dif_{\theta,\alpha}}$) from all the skymap sectors:

$$\mathbf{Dif_{tot} = \Sigma Dif_{\theta,\alpha}} \qquad \mathbf{(9)}$$

### *2.1.4 Global Solar Radiation Calculation*

Global radiation ($\mathbf{Global_{tot}}$) is calculated as the sum of direct and diffuse radiation of all sectors. The above processes are repeated for each location on the topographic surface, thus producing an insolation map for the whole study area.

$$\mathbf{Global_{tot} = Dir_{tot} + Dif_{tot}} \qquad \mathbf{(10)}$$

## 2.2 Design and Implementation of the Solar Analyst

**Overall Design:** The hemispherical viewshed algorithm and associated calculations were implemented in C++ library format, which can be flexibly loaded in other software in both PC and UNIX platforms. For PC use the program was compiled in Dynamic Link Library (DLL) format (solarlib.dll). There are three C++ classes in the calculation engine:

**The solar class** controls the main loop of the entire model. It reads the input DEM and calculates the horizon angles for each pixel in a DEM. Then it passes the horizon angles to the other two classes for the calculation of insolation. Finally, it gets the results and saves the results in files.

**The sun class** calculates local solar time, sun declination, sun position, sun rise/set time, day length, and solar constant. Also it calculates the day of year from solar declination values.

**The sky class** creates skymaps and sunmaps, converts horizon angles to viewsheds, overlays the skymaps and sunmaps with viewshed, and computes gap fraction and solar radiation for each sector.

The program is highly optimized and uses fast algorithms for computations, in particular, a fast line algorithm for searching maximum horizon angle, fast calculation of horizon angle, fast flood-fill function to assign identifications (visible versus obstructed) to sky regions in the viewshed, and fast overlay of the viewshed with sunmaps and skymaps. Also, the program creatively implemented calculations of partial sector information, penumbral effects, and dual sunmaps when needed to account for overlapping sunpaths for any period of time. To speed the calculation, instead of frequent access to a physical disk drive, calculations are performed mainly in the RAM. For example, the DEM is read into RAM when it is first opened and then used extensively for all subsequent viewshed calculations. The sunmaps and skymaps are created and stored in RAM, so they can be rapidly overlaid on viewsheds. The program has been extensively tested to assure its quality and stability.

Data input and output were implemented using the ArcView GridIO library (Fig 6), which comes with the ArcView Spatial Analyst. The user interface (Fig 7), which permits parameter input and calls the calculation engine, was developed using the ArcView Dialog Designer and Avenue. Because Avenue can not directly call C++ class member functions, another DLL, which calls the C++ member functions using nonmember functions, was developed as the interface between the calculation engine and Avenue. The Solar Analyst is based in ArcView, which supplies the Solar Analyst with its mapping, query, graphing and statistic analysis functions.

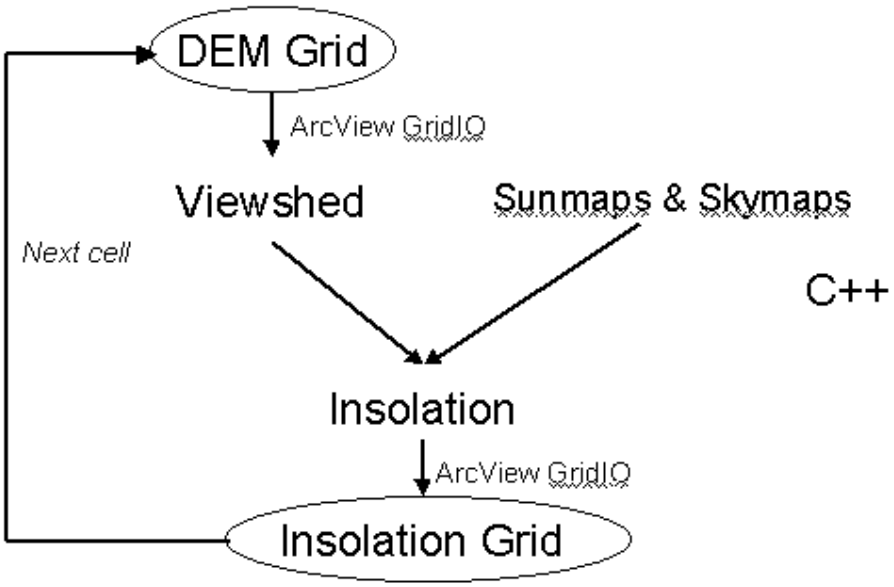


Fig. 6. Flow diagram showing the design of the Solar Analyst.

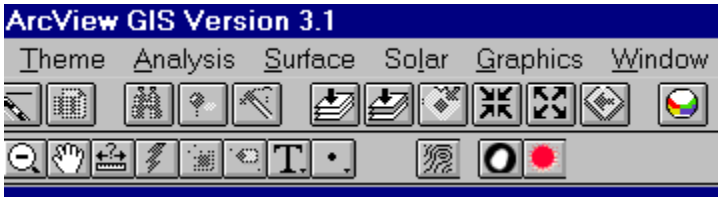


7A) Buttons and other tools allow calculation for interactively selected locations.

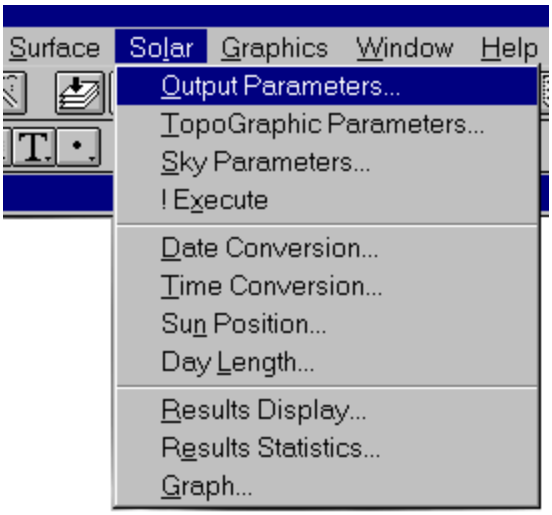


7B) Menus provide access to full capabilities.

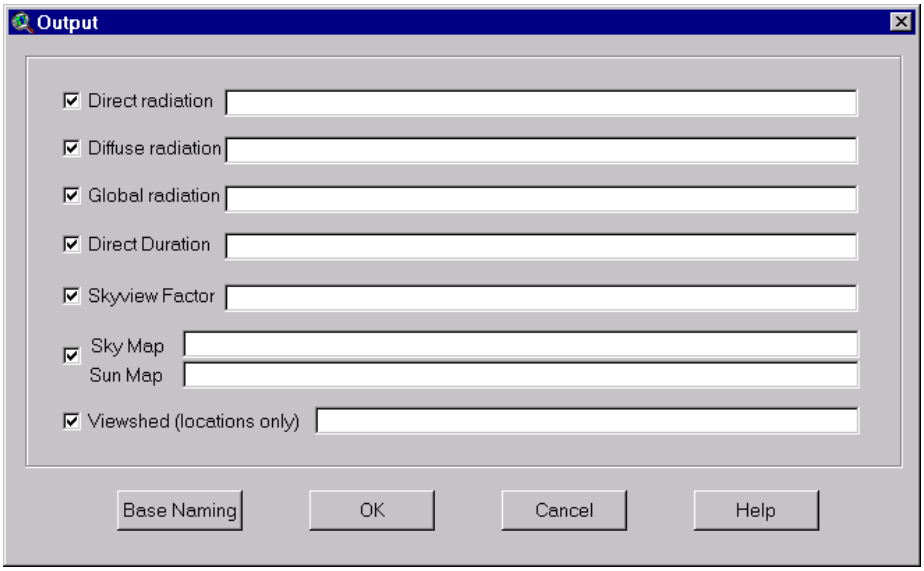


7C) The output dialog window permits specification of custom output.

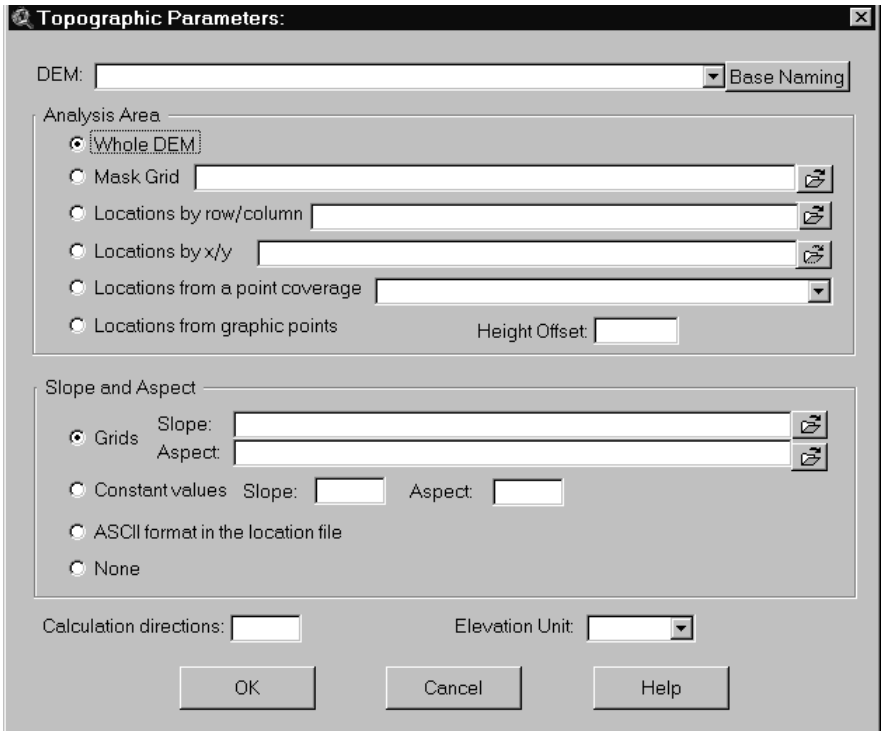


7D) The topographic parameter window permits specification of calculation parameters relevant to the topographic surface being analyzed.

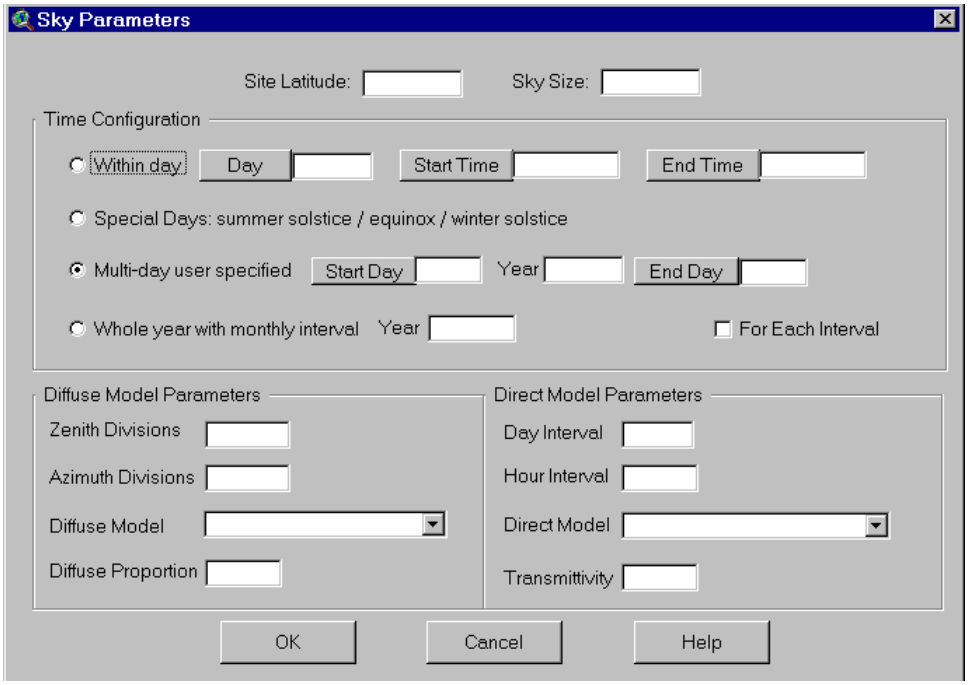


7E) The sky parameter window permits specification of parameters relevant to sunmap and skymap calculations.

Fig 7. User interface of the Solar Analyst.

**Program Specifications:** While the model algorithm appears somewhat complex, the Solar Analyst is designed to be easy to use. The Solar Analyst only requires a few input parameters and users do not need to have extensive knowledge of atmospheric physics or meteorology.

Output of the Solar Analyst includes the following:

- **Direct insolation**, **diffuse insolation**, **global insolation**, **direct radiation duration**, and **skyview factor** in Arc/Info Grid format or ASCII text format;
- **Skymaps** and **sunmaps** in Arc/Info Grid format;
- **Viewsheds** (for specific cells) in Arc/Info Grid format;
- **Horizon angles** in ASCII text format.

Input parameters to the Solar Analyst include the following:

- **DEM file name:** specifies an Arc/Info Grid file location. User has options to choose the following analysis areas:
    - **Whole DEM**.
    - **Area covered by a mask grid** (in Arc/info Grid format). For pixels near the edges of a DEM, the viewshed calculated may not be true because of the edge problems. Better results can be obtained if viewsheds are calculated only for areas away from the edge. This mask function is implemented for such purposes. While the Solar Analyst only calculates viewsheds for the masked area, it can use cells out of the mask grid boundary in calculating horizon angles.
    - **Locations by rows and columns** in ASCII format.
    - **Locations by x and y coordinates** in ASCII format.
    - **Locations from a point coverage** in Arc/Info coverage or shape file format,
    - **Locations of graphic points** in the view. This allows the user to specify points interactively and calculate the insolation or viewshed.
- **Object height offset:** this is used for location calculation only. For example, weather station sensors and solar powered devices are usually mounted above the ground.
- **Slope and aspect information:** users can choose from the following options:
    - **Grids:** as calculated from DEMs, or in some special cases provided by the user for a unique purpose.
    - **Constant values:** these values can be different from slope and aspect values calculated from the DEM. For example, solar radiation sensors are usually flat and mounted horizontally.
    - **ASCII files**: field surveys often measure slope and aspect for each sample location. These measured values are generally more accurate than DEM derived values. Using measured values can improve the accuracy of analysis.
    - **None:** perform calculations so that radiation values are corrected for angle of incidence. For example, some solar powered devices automatically change orientation to track the sun. In another example, a plant may have leaves in all orientations (random hemispherical distribution of orientations).

- **Directions for viewshed calculation:** because the viewshed calculation is highly intensive, horizon angles are only traced in the number of directions specified and horizon angles for other directions are calculated by interpolation.
- **Elevation unit:** in correction for air mass optical depth, the Solar Analyst performs calculations using elevation in meters. However, if the input DEM is in units other than meters, the program will convert the elevation into meters for calculations.

Sun/sky input parameters of the Solar Analyst include the following:

- **Site latitude:** this is used in such calculations as solar declination and solar position. Because the Solar Analyst is designed for landscape scales and local scales, it is acceptable to use one latitude value for the whole DEM.
- **Sky size:** this is the resolution for the viewshed, skymap, and sunmap.
- **Zenith and azimuth divisions:** these define the sky sectors of the skymap.
- **Diffuse radiation model:** currently users can choose either the uniform diffuse model or the standard overcast diffuse model.
- **Diffuse proportion:** the proportion of global normal radiation flux that is diffuse.
- **Transmittivity:** because the program will correct elevation effects, transmittivity should always be given for sea level. Also it is important to note the inverse relation between transmittivity and diffuse proportion when deciding values to use for calculations.
- **Time configuration**: the time for which insolation is to be calculated can be specified as follows:
  - **Within one day:** user can specify the day of year, starting time, and ending time. When starting time equals the ending time, instantaneous solar radiation is calculated.
  - **Special days:** for summer solstice, equinox, and winter solstice.
  - **Multi-day:** users can specify the start day, end day, year, day interval, and hour interval for calculations. When end day is smaller than start day, the end day is considered to be in the following year of the start day. A day interval of 7 corresponds with weekly intervals, whereas a day interval of 14corresponds with biweekly intervals.
  - **Whole year with monthly intervals:** this is a special multi-day calculation in that the day intervals are not constant.
  - **For each interval:** this check box gives users the flexibility to calculate total insolation or insolation for each session. For example, for multiple days with a day interval of 7, checking this box will create weekly insolation; otherwise, only the total insolation during the start day and end day are calculated. In another example, for within day with an hour interval of 1, checking this box will create hourly insolation calculations; otherwise, only the total insolation over the day is calculated.

## 3. METHODS

### 3.1 Study Site

We have been applying the Solar Analyst in our research concerning microclimate and vegetation patterns in the vicinity of the Rocky Mountain Biological Lab (RMBL), Colorado. Dramatic topographic variation, with elevations ranging from 2532 m to 4340 m, leads to a diversity of vegetation communities (Langenheim 1962).

### 3.2 Weather Stations & Insolation Monitoring

Four weather stations have been established in the vicinity of RMBL (Fig. 8). One weather station (called the "research meadow" station) was established in 1989 by the Environmental Protection Agency. The other three (called the "upper meadow", "middle meadow", and "lower meadow" stations) were established in June 1997 for research concerning climate change and include monitoring of global insolation using Li-Cor pyranometers mounted horizontally about 2 m above the ground (John Harte unpublished). Readings were averaged and recorded using a Campbell data logger at hourly intervals during summer of 1997 and at two-hour intervals thereafter.

### 3.3 Digital Elevation Model

We constructed a DEM for the vicinity of RMBL using 30-m resolution DEMs for nine U.S. Geological Service 7.5' quadrangles: Gothic, Snowmass Mt., Maroon Bells, Hayden Peak, Oh-Be-Joyful, Pearl Pass, Axtell, Cement Mt., and Crested Butte. The RMBL vicinity DEM was used to calculate viewshed and insolation. Locations of the weather stations were surveyed using a differentially corrected Global Positioning System (Trimble Pathfinder). Both the RMBL vicinity DEM and the weather station locations were converted into a Universal Transverse Mercator projection (Fig. 8).

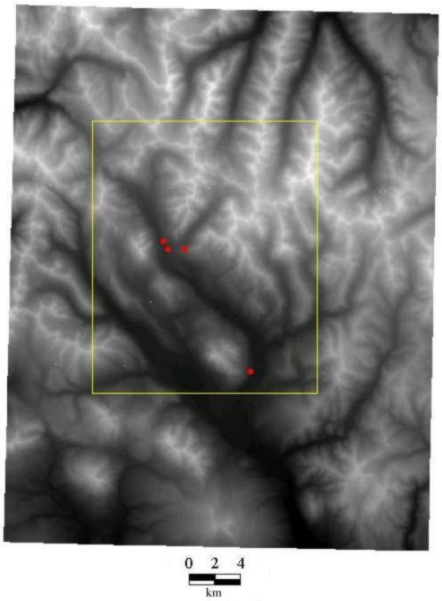


Fig. 8. RMBL vicinity DEM, weather station locations (red) and calculation mask (yellow).

### 3.4 Viewshed Calculation and Hemispherical Photographs

Viewsheds were calculated for each location within the calculation mask (fig 8). We compared the calculated and observed viewsheds for each weather station using hemispherical photographs taken near the insolation sensor. For viewshed calculations a 2m offset was added to account for the height of the sensor and horizon angles were calculated at 64 directions.

### 3.5 Insolation Patterns

**Temporal Patterns through the Day:** Insolation on a typical clear day, July 4, 1997, was calculated and compared with sensor values for the "middle meadow" site. The sensor measurements were converted to true local solar time using the equation for time to account for the time zone meridian. Calculations used a transmittivity value of 0. 6 and a diffuse proportion of 0. 2. Slope was set to zero, corresponding to the horizontal surface of the insolation sensor. The viewshed was calculated along 64 directions to obtain good accuracy; sky size was set at 512 x 512 cells; the skymap was created using 18 zenith divisions and 16 azimuth divisions; and the sunmap was created using a 6-minute (0.1 hour) interval through the day.

**Annual Insolation Patterns:** Monthly insolation was calculated throughout the course of the year for the "research meadow" site assuming transmittivity of 0.5 and diffuse proportion of 0.3. Again slope and aspect were set to zero, the viewshed was calculated along 64 directions, sky size was set at 512 x 512 cells, and the skymap was created using 18 zenith divisions and 16 azimuth divisions. The sunmap was created using half-hour intervals through the day and monthly intervals through the year.

**Spatial Patterns of Insolation:** The Solar Analyst was used to calculate monthly direct, diffuse, global, and direct duration maps from the RMBL DEM (4 maps x 12 months = 48 maps total). The program was run on a Compaq Armada 7800 (333MHz CPU and 128M RAM). Parameters were set to transmittivity of 0. 5, diffuse proportion of: 0. 3, 32 viewshed calculation directions, a sky size of 200 x 200, a skymap of 8 zenith divisions and 8 azimuth divisions, and a sunmap of half-hour intervals through the day and monthly intervals through the year. The DEM consists of 1,591,590 (1410 x 1113) grid cells. To avoid edge effects, insolation was only calculated for the center area by applying a mask of 703 x 574 (403,522) cells (Fig. 8). When calculating viewshed, the pixels out of the mask were still used to calculate horizon angles.

### 3.6 Inferring Insolation from Incomplete Data

A variety of approaches have been employed when insolation data are incomplete or unavailable. Based on our temporal and spatial analyses we examine the validity of various of these approaches:

- **Using measurements from nearby monitoring stations to infer insolation for a broader area:** A histogram was constructed to permit examination of the extent of spatial variation in annual global insolation, based on the direct and diffuse maps of insolation for the study area.

- **Grouping aspect and slope:** Summary statistics of insolation for the month of June (minimum, maximum, and mean) were calculated for six categories of slope and aspect in the study area: aspects of north vs. south and slopes of 0-29$^{o}$, 30-59$^{o}$, and 60-90$^{o}$. These statistics permit examination of the validity of using such categories.
- **Using sinusoidal curves to simulate daily insolation patterns:** Daily insolation curves were calculated for four locations with different aspects (north-, south-, east-, and west-facing) to examine the influence of orientation on the shape of the daily insolation curve.
- **Calculating diffuse solar radiation as a proportion of direct or global solar radiation:** The same daily insolation curves for locations with different aspects, along with their viewsheds, were used to examine the validity of calculating diffuse radiation as a proportion of direct or global measurements from sensors.
- **Using direct duration to estimate direct insolation:** We calculated correlation coefficient between direct duration and direct, diffuse, and global radiation for each month based on the insolation maps for the study area.

### 3.7 Sensitivity Analysis

A series of sensitivity analyses were used to assess the effects of different input parameters on the outputs from the Solar Analyst:

- **Viewshed Calculation Directions:** To assess tradeoffs between calculation speed and accuracy, we tested the sensitivity of the Solar Analyst to different numbers of calculation directions using the RMBL DEM (a topographically complex area) and another DEM in Kansas (a low-relief area). For each of the two DEMs, horizon angles for three locations were computed at 8, 16, 24, 32, 40, 64, 128 and 360 directions. Calculated viewsheds were compared with the 360-direction viewshed.
- **Sky resolution and skymap divisions:** To assess tradeoffs between calculation speed and accuracy, we tested the sensitivity of the Solar Analyst to two sets of sky resolution and skymap divisions: 400 x 400 sky size with 16 x 16 skymap divisions and 200 x 200 size with 8 x 8 skymap divisions.
- **Sunmap divisions:** To assess tradeoff between calculation speed and accuracy, we tested the sensitivity of the Solar Analyst to various combinations of sunmap divisions, ranging from 0.2 to 1.0 hour intervals through the day and between one day and one month intervals through the year.
- **Elevation effects:** We assessed the importance of elevation corrections in the Solar Analyst by examining relations between elevation, optical air mass, and insolation.

## 4. RESULTS AND DISCUSSION

### 4.1 Viewsheds

The calculated and observed viewsheds match well (Fig. 9). The strongest correspondence between calculated and observed viewsheds are for more distant features, such as Gothic Mountain to the west and Whiterock Mountain to the northeast. Small discrepancies exist toward

the north and east because of trees. In some cases such discrepancies can be more pronounced either due to strong effects of nearby features such as trees or errors inherent in a DEM.

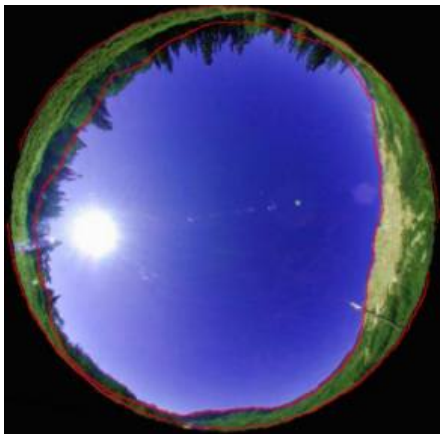

Fig. 9 Comparison of calculated viewshed with a hemispherical photo

### 4.2 Insolation Patterns

**Temporal Patterns through the Day:** There is excellent agreement between the measured and calculated global insolation values through the day (Fig. 10). Total insolation for the "middle meadow" site on July 4, 1997 was observed to be 8115. 4 w/m$^{-2}$, of which direct was 6967.2 w/m$^{-2}$ (85.9%) and diffuse was 1148.3 w/m$^{-2}$ (14.1%). Note that that insolation values jump at about 6:15 and drop around 17:20. This results from the geometry of the viewshed, as can clearly be seen by referring back to Fig. 8. The geometry of sky obstruction allows us to predict when direct radiation drops off. Before 6:15 sky obstruction by Whiterock Mountain blocked direct radiation and only the diffuse radiation component contributed to global radiation. At about 17:20 the sun was blocked by Gothic Mountain and the global insolation was again reduced to only the diffuse radiation component.

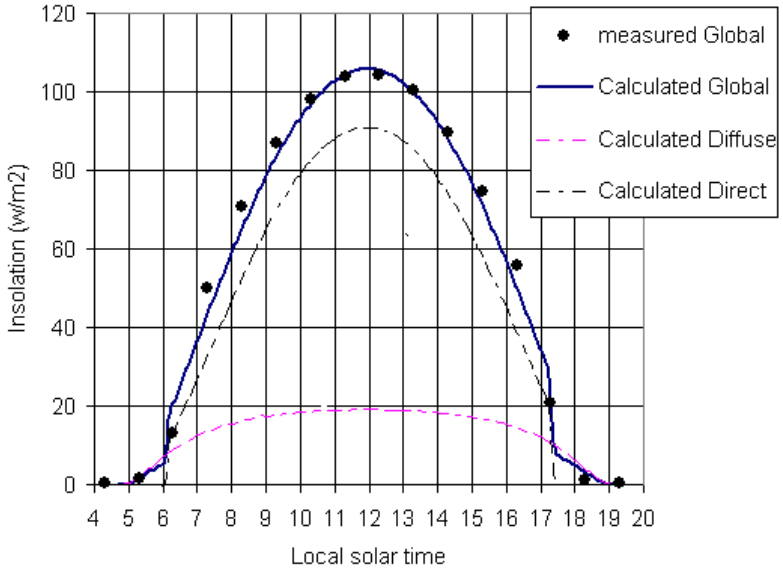


Fig. 10 Comparison of calculated and observed insolation for typical clear day

**Annual Insolation Patterns:** The annual pattern of monthly insolation for the "research meadow" site displays a distinct sinusoidal pattern, with a peak near the summer solstice and a trough near the winter solstice (Fig. 11). This pattern is driven primarily by the shifting angle of the suntrack with respect to the horizontal surface of interception. In the field considerable variation exists from one day to another and from one year to another, caused mainly by variation in cloud cover. The Solar Analyst is able to calculate insolation for different atmospheric conditions, but information about variation in transmittivity and diffuse proportion parameters are not typically available. The Solar Analyst can only be used to examine short-term non-systematic variation in cases where detailed insolation monitoring is available for the region of interest. More commonly, the Solar Analyst is best suited for comparing daily patterns and seasonal patterns as they vary spatially.

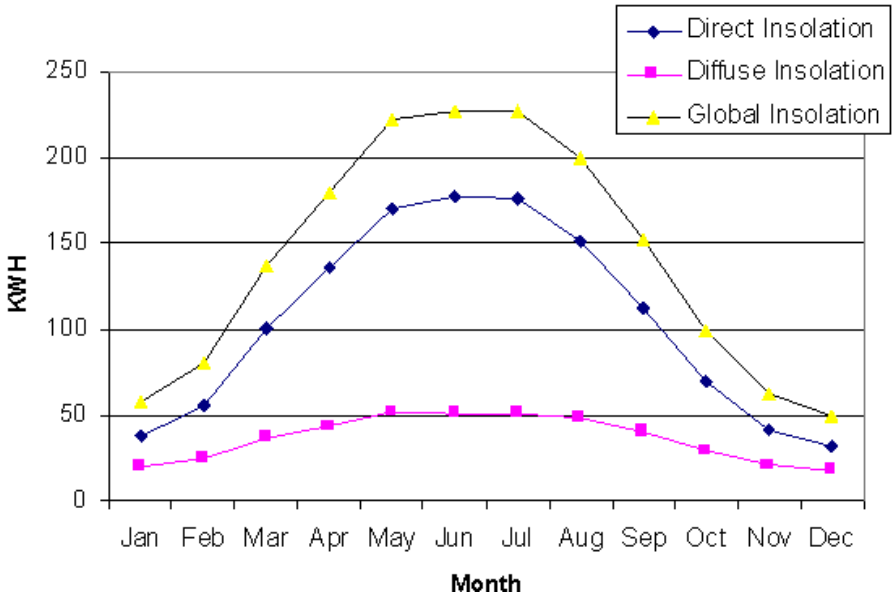


Fig. 11 Annual pattern of direct, diffuse and global insolation for average clear day for the weather station at the research meadow

**Spatial Patterns of Insolation:** It required three hours to calculate the monthly direct, diffuse, global, and direct duration maps (48 maps total). Maps of direct and diffuse insolation for the whole year are shown in Figs. 12 and 13. Among the distinct patterns that can be observed by inspection of the annual direct radiation map (Fig. 12) are distinctly lower insolation on north-facing slopes as compared with south-facing slopes, as well as lower insolation levels in landscape positions with high sky obstruction along the suntrack (i.e., mountains toward the south, east, or west). By contrast, variation in the annual diffuse insolation map results primarily as a function of slope (higher slope causing lower values) and sky obstruction in any direction (more sky obstruction causing lower values).

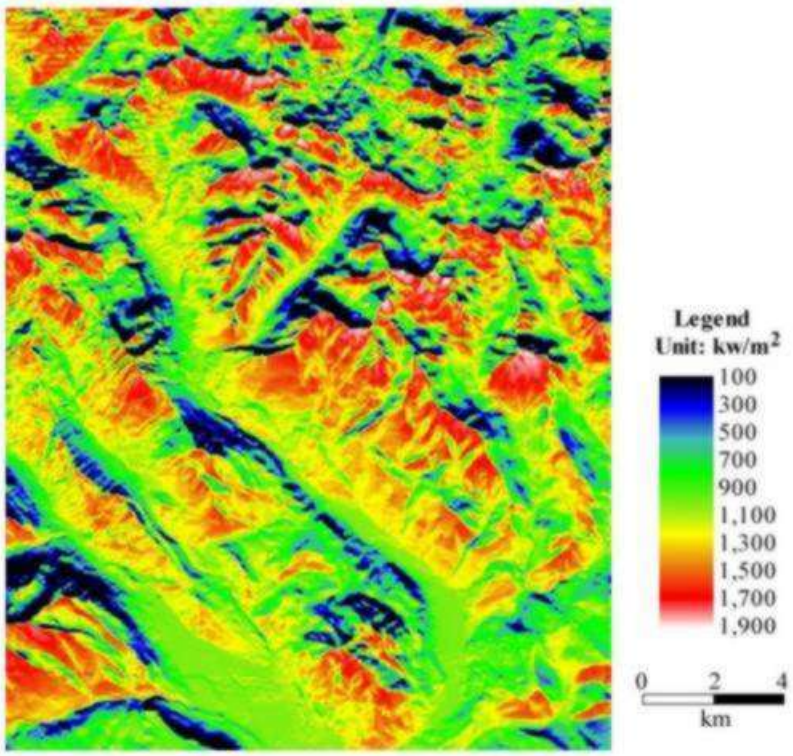


Fig 12. Map of annual direct insolation (note map quality reduced because of file compression)

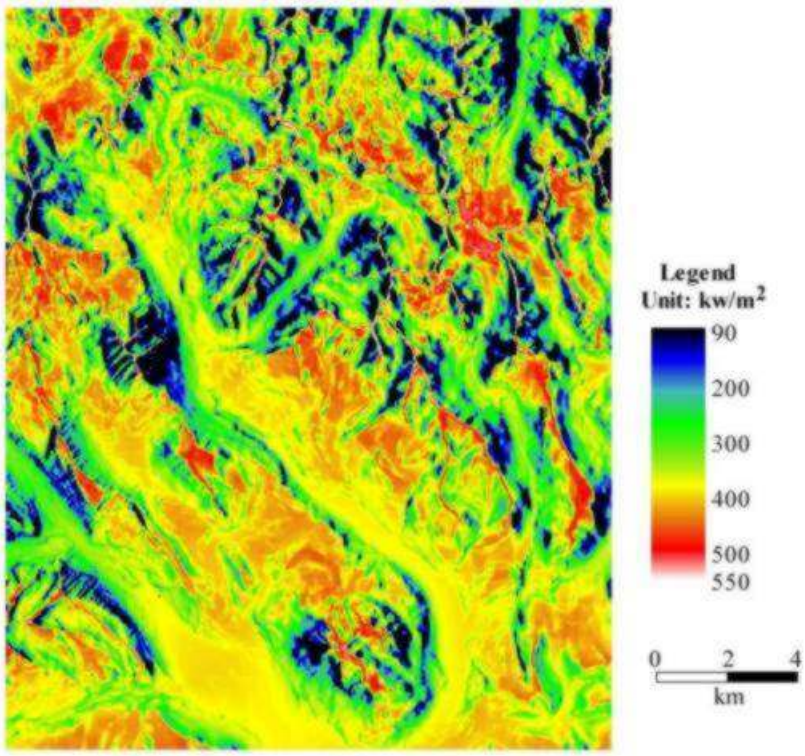


Fig 13. Map of annual diffuse insolation (note map quality reduced because of file compression)

### 4.3 Inferring Insolation from Incomplete Data

**Using measurements from nearby monitoring stations to infer insolation for a broader area:** Commonly studies use measurements at one weather station to infer patterns for the entire study area. This approach can neglect the temporal and spatial variation of insolation. In many situations, especially for mountainous regions, this approach is not effective. Tremendous variation exists in insolation received at different spatial locations (Fig. 14). In this example, the variation results directly from variation in topography. Additional variation in insolation can result because of spatial variation in atmospheric conditions, in particular cloud cover.

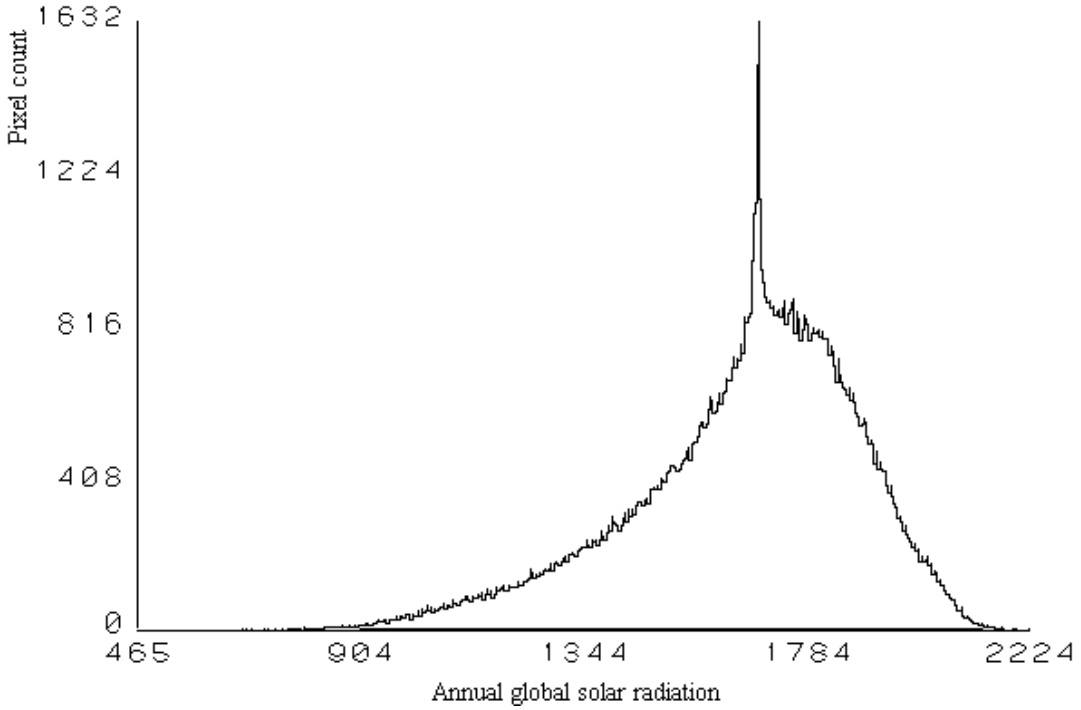


Fig 14. Variation of annual insolation (KWH/$m^2$) over the study area.

**Grouping aspect and slope:** Commonly locations with similar slopes and aspects are grouped in analysis to infer variation of insolation in the landscape. In the northern hemisphere it is generally assumed that south-facing slopes receive more insolation than north facing slopes, while the converse is assumed in the southern hemisphere. While south-facing slopes do have mean insolation values higher than north-facing slopes during the month of June (Table 1), the statistic demonstrate that there are many cases where north-facing slopes receive more insolation than south-facing slopes. This results because of local sky obstruction and the importance of early and late times during the day when the suntrack is far to the north.

Table 1.Summary statistics, according to aspect and slope category, for insolation values in June (KWH/$m^2$).

| Aspect | Slope | Min | Max | Mean |
|---|---|---|---|---|
| North | 0-29 | 146 | 257 | 218 |
| | 30-59 | 90 | 253 | 183 |
| | 60-90 | 95 | 108 | 101 |
| South | 0-29 | 138 | 261 | 219 |
| | 30-59 | 90 | 263 | 192 |
| | 60-90 | 99 | 167 | 141 |

**Using sinusoidal curves to simulate daily insolation patterns:** Symmetrical sinusoidal curves have been widely used to simulate daily insolation patterns. Symmetrical daily patterns generally only can occur for flat surfaces or aspect directly north or south, and with symmetrical east-west sky obstruction. Asymmetrical daily insolation results from slope orientation to the east or west and from asymmetrical sky obstruction (Fig. 15). Further asymmetry of daily insolation patterns can result from variation in atmospheric conditions, for example in locations where afternoon clouds are common.

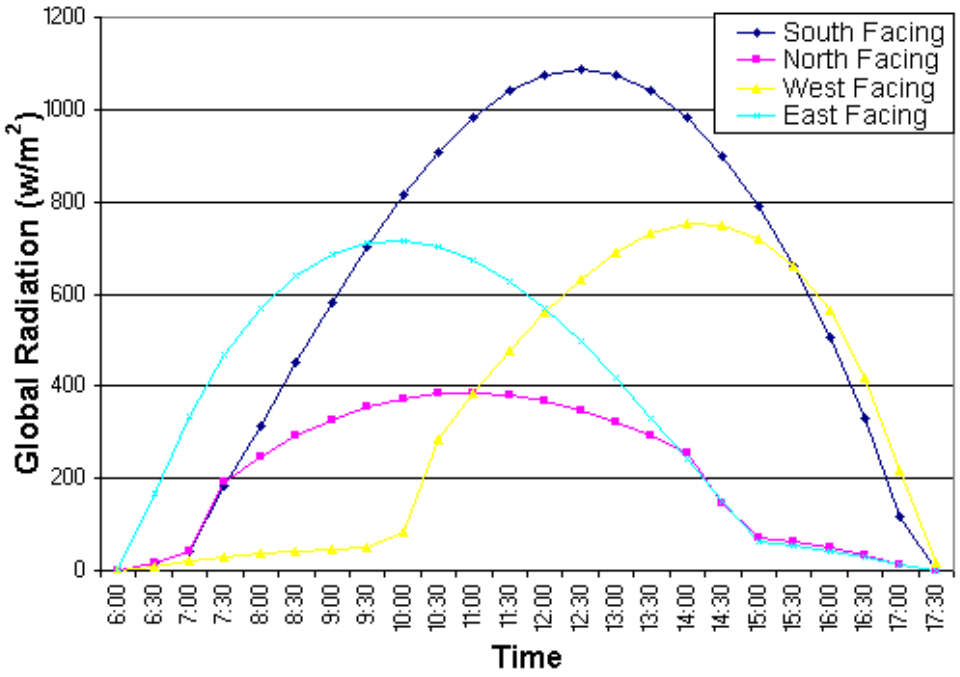


Fig 15. Daily Insolation patterns for locations on different slopes.

**Calculating diffuse solar radiation form direct or global solar radiation:** Various relations between diffuse and global or direct model has been formulated (Liu and Jordan 1960, Erbs 1980). These models are used to calculate diffuse radiation components when only global radiation striking a horizontal sensor is measured, or when only direct insolation is calculated. These models assume relations between diffuse and global or direct radiation without considering differences in viewsheds. Further, these models have been widely used, even in mountainous regions, to derive daily or seasonal insolation patterns. A western slope may have as much as 100% diffuse radiation in the morning while only 15% diffuse radiation in the afternoon (Fig. XX). Similarly, some slopes may have 100% diffuse radiation during the entire winter season, but with a low proportion of diffuse radiation in the summer. High variability in slope orientation and viewsheds mean that this approach is generally not valid.

**Using direct duration to estimate direct insolation:** In the absence of solar radiation measurements, it is common practice to use direct duration as an estimate of direct insolation. Correlations between duration and direct measurements are higher in winter than in summer; while correlations between duration and diffuse measurements are higher in summer than in winter (Table 2). Correlations between duration and global measurements are higher in winter than in summer, but correlations can be as low as 0.41. The primary problem of using direct duration to predict insolation is that it does not account for either the angle of incidence or the length of the atmosphere traversed, both of which vary markedly through the day.

Table 2. Correlation between direct duration and radiation

| | Duration & Global | Duration & Direct | Duration & Diffuse |
|---|---|---|---|
| Jan | 0.7153 | 0.6922 | 0.3740 |
| Feb | 0.6642 | 0.6281 | 0.4714 |
| Mar | 0.5287 | 0.4567 | 0.6305 |
| Apr | 0.4128 | 0.2947 | 0.6929 |
| May | 0.4337 | 0.2954 | 0.6743 |
| Jun | 0.4576 | 0.3290 | 0.6640 |
| Jul | 0.4273 | 0.2927 | 0.6672 |
| Aug | 0.4226 | 0.2916 | 0.6914 |
| Sep | 0.4881 | 0.3995 | 0.6684 |
| Oct | 0.6386 | 0.5925 | 0.5200 |
| Nov | 0.7159 | 0.6907 | 0.3880 |
| Dec | 0.7352 | 0.7175 | 0.3343 |

### 4.4 Sensitivity Analysis

**Viewshed Calculation Directions:** A set of 32 calculation directions were sufficient to obtain a mean error less than 0.5 degree for the complex mountain topography around RMBL. By contrast, only 8 or 16 directions were needed to obtain a mean error less than 0.5 degree for the gentle topography in Kansas. are needed for such complex mountain topography as RMBL. Because horizon angle calculation is computationally intensive, users should select the minimum set of azimuth directions that suit their needs. Horizon angles at other directions are calculated using simple linear interpolation.

**Sky resolution:** Similar results were obtained using 400 x 400 and 200 x 200 sky resolution. are highly similar. The correlation between the calculated global insolation is 0. 99994 at winter and 0.99995 at summer. The average value differs by less than 1%. Based on this testing, we concluded that a 200 x 200 sky size is sufficient for most purposes. Increasing sky size beyond this does not significantly improve model accuracy, but greatly increases computation time. For example, doubling the sky resolution from 200 x 200 to 400 x 400 quadruples the computation time. The Solar Analyst is implemented such that sky resolution is user defined. Further research may reveal cases where higher sky resolutions may be required.

**Skymap divisions:** Increased number of skymap divisions does not affect computation time greatly and does not improve global radiation much as shown in the above test. The results because diffuse radiation is generally a relatively small proportion of global radiation, and because we are using uniform sky or standard overcast models. In most situations 8 x 8 sky divisions is sufficient. In cases where diffuse radiation is of major interest, skymap divisions should be increased to 16 x 16 or even more. Skymaps of 18 zenith divisions (5-degree intervals) and 16 azimuth divisions (22.5-degree intervals) are commonly employed for detailed studies (Rich et al. 1999).

**Sunmap divisions:** Changing sunmap divisions does not change computational time much, but can improve calculation accuracy. In general, a 0.2 hour interval through the day is sufficient for daily insolation calculations, and a 0.5 hour interval is sufficient for multi-day calculations. The appropriate interval through the year is usually determined based on user needs. For example, it should be 7 for weekly calculations, 14 for biweekly calculations, and monthly for monthly calculations.

**Elevation effects:** Generally, higher elevations receive more insolation than lower elevations. This results both because higher elevation have more open viewsheds and because the solar beam travels through less air mass (Fig. 16). For the vicinity of RMBL, the air mass is approximately half at the upper most elevation ( 4,340 m) as compared with the lowermost elevation (2,532 m). While a change of 10 m has trivial effects on air mass and insolation, a change from sea level to 5,000 m can result in an increase of 52% in global radiation (Table 2). Another effect that partially counterbalances less air mass at higher elevations involves increased cloudiness with increasing elevation.

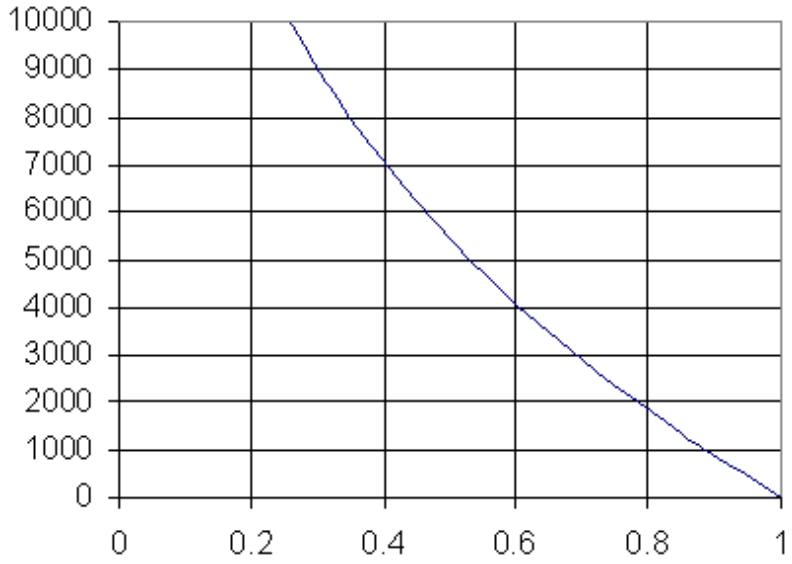


Fig 16. The relationship between elevation and zenith air mass optical depth.

Table 3. Effects of elevation on insolation

| Elevation (m) | Relative air optical depth at zenith | Insolation ($w/m^2$) at average clear day Flat and open surface at latitude 38.95N, 12:00pm at equinox | | |
|---|---|---|---|---|
| | | Direct | Diffuse | Global |
| 0 | 1 | 435.9 | 120.2 | 556.1 |
| 10 | 0.999 | 436.3 | 120.4 | 556.7 |
| 1000 | 0.89 | 482.0 | 132.9 | 614.9 |
| 2000 | 0.78 | 528.1 | 145.7 | 673.8 |
| 3000 | 0.69 | 573.8 | 158.3 | 732.1 |
| 4000 | 0.60 | 618.4 | 170.6 | 789.0 |
| 5000 | 0.53 | 661.4 | 182.4 | 843.9 |

### 4.5 DEM Issues

**DEM Quality:** DEMs are used to derive three kinds of information: elevation, slope and aspect, and viewsheds. Their effects on model accuracy can be assessed in separately:

- **Elevation:** Elevation is used directly in calculation of air optical depth. Though, elevation can deviate significantly from actual values, a 10 to 30 m error will only affect the air

optical depth at 0.1%. Thus elevation errors do not produce significant effects on model accuracy.

- **Slope and aspect:** Poor DEM quality, limitations due to resolution, and edge effects can lead to inaccurate slopes and aspects. This is a potentially serious source of error because insolation values are corrected for angle of incidence, which ultimately depends on surface slope and aspect. The Solar Analyst has the ability to use surveyed slopes and aspects, which can improve accuracy for various applications.

- **Viewsheds:** Based on our experience, DEM does not generally change viewsheds greatly, however further work is needed to assess cases where viewshed errors may be significant.

One important index of DEM quality is its cell size. As grid cell increases, topographic generalization occurs. While the average regional radiation may not change much, values for some individual cells may change significantly. The quality of DEMs, including the cell size, should be evaluated against user needs. The commonly available 30 m USGS DEM is sufficient for most environmental and ecological applications at landscape scales. Applications that require high accuracy for specific locations may require higher resolution DEMs.

**DEM Projection Considerations:** For viewshed calculations, the Solar Analyst assumes DEMs are in a projection that preserves direction. Most DEMs are available in projections that do not exactly preserve direction. For some commonly used projections (e.g. UTM), slight rotation of the study area to register correctly with true north can be sufficient to improve accuracy.

### 4.6 Limitations

**Clouds:** The Solar Analyst does not currently model clouds, per se, although clouds can be taken into account when estimating transmittivity and diffuse proportion. Clouds are extremely hard to model or predict, and detailed information, such as clouds distribution, thickness, cloud type, are not available for most areas. If such data are available, the Solar Analyst could readily be customized by adding a cloud skymap that can be overlaid with the viewshed, skymap, and sunmap. Alternatively cloud information could be included in specification of sector-specific insolation when construction skymaps and sunmaps. For many purposes, in particular involving multi-day insolation calculation, cloud effects can be included by using an appropriate transmittivity and diffuse proportion.

**Reflected Radiation:** The Solar Analyst currently neglects the contribution of reflected radiation from the ground. This is valid for most uses. Reflected radiation is important for places where ground surfaces have high albedo, for example, snow-covered surfaces. Reflected radiation is complex because it varies with surface cover properties, surface orientation, and sun position. However, the algorithm utilized in the Solar Analyst permits calculation of simplified estimations of reflected radiation (Rich 1994). In the viewshed, direct and diffuse radiation come from visible sky directions, while ground-reflected radiation comes from obstructed directions. We can assign obstructed sky sectors a reflectance index that estimates the reflectance from ground features. The reflected radiation can then be calculated by summing the reflected radiation from obstructed sectors in a manner similar to the way direct and diffuse radiation

calculated. Locations open to lower surfaces can receive reflected radiation from lower elevations. In these cases a hemispherical view downward could be used to account for upwelling radiation. In general, implement this approach is challenging.

**Ground Features:** Generally, a DEM only describes the topographic terrain and does not represent ground features such as plant canopies and human structures. Such ground features can have a, which can affect ground insolation strongly. If these ground features can be included in DEMs the Solar Analyst can still be used. For example, in urban areas it is possible to construct a high-resolution DEM that including buildings and other structures. Irregular features, such as plant canopies can also be converted into DEMs, but obtaining such data can be challenging (Rich et al. 1993, Price et al. 1995). For detailed characterization of specific locations, hemispherical photography can be a more appropriate technique (Rich 1989, 1990, Rich et al. 1999). With minor modification, the calculation engine of the Solar Analyst can use hemispherical photography to examine solar radiation regimes for specific locations. Further work is needed to fully integrate the Solar Analyst with spatially explicit canopy models such as those of Fournier et al. (1997).

## 4. CONCLUSION

In the development of the Solar Analyst, we implemented a fast and effective algorithm that permits accurate calculation of topographic influences on solar radiation over local and landscape scales. Considerable insolation variation exists between different landscape positions. Such variations have a significant effect on the ground energy balance, water balance, and nutrient cycles, which directly or indirectly affect natural processes and human activities. As an example of its application, we are using the Solar Analyst and meteorologic measurements in models of spatial patterns of microclimate factors, including air temperature, soil temperature, and soil moisture. This topoclimatic modeling approach can lead us to a better understanding of the relationship between microclimate and vegetation distribution patterns, as well as potential habitat shifts under climate change scenarios. Preliminary analyses demonstrate that commonly used techniques (generalization from nearby insolation monitoring, prediction by slope and aspect categories, estimating direct radiation from direct duration, etc.) are not sufficiently accurate for generalization of insolation patterns to a landscape scales. The Solar Analyst serves as a powerful tool for analyzing spatial and temporal patterns of insolation at local and landscape scales. Applications span a broad range of fields, including forestry, agriculture, hydrology, micrometeorology, environmental assessment, and ecological research. The Solar Analyst also promises to be useful in engineering and design fields, for such applications such as site assessment, building design, solar collector design, and topographic radiometric correction for remote sensing.


### ACKNOWLEDGEMENTS

This research was supported by the Information Telecommunication and Technology Center (ITTC), the Kansas Biological Survey, the University of Kansas General Research Fund, and Helios Environmental Modeling Institute. We would like to give thanks to Susannah Geer for

providing editorial comments and field assistance and to Brett Greene for providing field assistance. We also thank John Harte, Jennifer Dunne, and Marc Fischer at the University of California, Berkeley, who provided weather and other environmental data, gathered with support from National Science Foundation grants DEB-96-2889 and DEB-96-23258 to John Harte.

## REFERENCES

Buffo, J., L.J. Fritschen, and J.L. Murphy. 1972. Direct solar radiation on various slopes from 0° to 60° north latitude. *U. S. Forest Service Pacific Northwest Forest Range Experimental Station Research Paper,* PNW-142.

Dozier, J. and J. Frew. 1990. Rapid calculation of terrain parameters for radiation modeling from digital elevation model data. *IEEE Transactions on Geoscience and Remote Sensing* 28:963-969.

Dubayah, R. and P.M. Rich. 1995. Topographic solar radiation models for GIS. *International Journal of Geographic Information Systems* 9:405-413.

Dubayah, R. and P.M. Rich. 1996. GIS-based solar radiation modeling. pp. 129-134 In: M.F. Goodchild, L.T. Steyaert, B.O. Parks. C. Johnston, D. Maidment, M. Crane, and S. Glendinning (eds). *GIS and Environmental Modeling: Progress and Research Issues*. GIS World Books. Fort Collins, CO.

Erbs, D.G., S.A. Klein and J.A. Duffie. 1982. Estimation of the diffuse radiation fraction for hourly, daily, and monthly-average global radiation. *Solar Energy* 28:293-302.

Flint, A.L. and S.W. Childs. 1987. Calculation of solar radiation in mountainous terrain. *Agriculture and Forest Meteorology* 40:233-249.

Fournier, R.A., P.M. Rich, and R. Landry. 1997. Hierarchical characterization of canopy architecture for boreal forest. *Journal of Geophysical Research, BOREAS Special Issue* 102(D24):29445-29454.

Frank, E.C., and R. Lee. 1966. Potential solar beam irradiation on slopes: Tables for 30° to 50° latitude. *U. S. Forest Services Rocky Mountain Forest Range Experimental Station Paper* RM-18.

Geiger, R.J. 1965. *The climate near the ground*. Harvard University Press, Cambridge.

Gates, D.M. 1980. *Biophysical Ecology.* Springer-Verlag, New York.

Hetrick, W.A., P.M. Rich, and F.J. Barnes, and S.B. Weiss. 1993a. GIS-based solar radiation flux models. *American Society for Photogrammetry and Remote Sensing Technical Papers, Vol 3, GIS Photogrammetry and Modeling*. pp. 132-143.

Hetrick, W. A. , P. M. Rich, and S. B. Weiss. 1993b. Modeling insolation on complex surfaces. *Thirteen Annual ESRI User Conference*, Volume 2, pp. 447-458.

Iqbal, M. 1983. *An Introduction to Solar Radiation*. Academic Press, N. Y. , pp:1-28.

Kondrtyev, K.Y. 1969. *Radiation in the Atmosphere.* New York: Academic Press.

Kumar, L., A.K. Skidmore and E. Knowles. 1997. Modeling topographic variation in solar radiation in a GIS environment. *International Journal of Geographic Information Science,* 11:475-497.

Langenheim, J.H. 1962. Vegetation and environmental patterns in the Crested Butte Area, Gunnison, Colorado. Ecological Monographs 32:249-285.

List, R.J. 1971. *Smithsonian meteorological tables*, Sixth revised edition, Smithsonian Miscellaneous Collections. Volume 114. Smithsonian Institution Press. Washington.

Liu, B.Y. and R.C. Jordan. 1960. The interrelationship and characteristic distribution of direct, diffuse and total solar radiation, *Solar Enerdy*, 4:1-19.

Pearcy, R.W. 1989. Radiation and light measurements. pp. 95-116. In: R.W. Pearcy, J. Ehleringer, H.A. Mooney, and P.W. Rundel (eds). *Plant Physiological Ecology: Field Methods and Instrumentation*. Chapman and Hall. New York.

Price, K.P., P.M. Rich, and R.L. O'Neal. 1995. Deriving high resolution canopy digital elevation models. *American Society for Photogrammetry and Remote Sensing Technical Papers, Vol. 2*. pp 281-289.

Rich, P.M., J. Wood, D.A. Vieglais, K. Burek, and N. Webb. 1999. *Guide to HemiView: software for analysis of hemispherical photography*. Delta-T Devices, Ltd., Cambridge, England.

Rich, P.M., W.A. Hetrick, and S.C. Saving. 1995. *Modeling Topographic Influences on Solar Radiation: a manual for the Solarflux model*. Los Alamos National Laboratory Report LA-12989-M.

Rich, P.M., R. Dubayah, W.A. Hetrick, and S.C. Saving. 1994. Using Viewshed models to calculate intercepted solar radiation: applications in ecology. *American Society for Photogrammetry and Remote Sensing Technical Papers*, pp 524-529.

Rich, P.M., G.S. Hughes, and F.J. Barnes. 1993. Using GIS to reconstruct canopy architecture and model ecological processes in pinyon-juniper woodlands. *Thirteenth Annual ESRI User Conference, Volume 2*. pp. 435-445.

Rich, P.M. 1990. Characterizing plant canopies with hemispherical photography. In: N.S. Goel and J.M. Norman (eds). Instrumentation for studying vegetation canopies for remote sensing in optical and thermal infrared regions. *Remote Sensing Reviews* 5:13-29.

Rich, P.M. 1989. *A manual for analysis of hemispherical canopy photography*. Los Alamos National Laboratory Report, LA-11733-M.

Swift, L.W. 1976. Algorithm for solar radiation on mountain slopes. *Water Resources Research* 12:108-112.